

## SUPPLEMENTARY MATERIAL TABLE OF CONTENTS

SUPPLEMENTARY METHODS .....	2
Mouse procedures and reagents .....	2
Mouse model of myocardial ischemia–reperfusion injury .....	2
Quantification of infarct size .....	3
Myocardial neutrophil infiltration .....	3
Transwell assay of chemokine-induced migration .....	4
Thioglycolate-induced peritonitis .....	4
LPS-induced acute lung inflammation .....	5
Lung processing for histology and immunofluorescence .....	5
Flow cytometry .....	6
Immunoblotting .....	7
Confocal microscopy .....	7
Intravital microscopy .....	7
Tracking of crawling neutrophils .....	8
Neutrophil–platelet interactions .....	9
3D reconstruction of polarized neutrophils .....	9
In-silico modeling of mouse and human $\beta$ 1AR and comparative ligand docking .....	10
Statistics .....	11
SUPPLEMENTAL FIGURES .....	12
Supplemental Fig. 1. Dose response hemodynamic study in mice .....	12
Supplemental Fig. 2. Pre-reperfusion intravenous metoprolol does not affect the percentage and number of neutrophils 24 h post-IRI .....	13
Supplemental Fig. 4. Metoprolol reduces MPO and ameliorates ALI .....	16
Supplemental Fig. 5. Bioinformatics Pipeline for the in-silico model of the mouse and human $\beta$ 1AR proteins and for the simulation of the docking of these models with four ligands: epinephrine, metoprolol, atenolol or propranolol. ....	18
Supplemental Fig. 6. Metoprolol induces a conformational change in mouse $\beta$ 1AR that increases the size of the intracellular cavity .....	19
SUPPLEMENTAL TABLES .....	21
Suppl. Table 1. Quantification of complex and interface energies of ligand-human $\beta$ 1AR interaction....	21
Suppl. Table 2. Quantification of conformational change in binding pocket and intracellular cavity upon ligand-human $\beta$ 1AR interaction. ....	21
Suppl. Table 3. Quantification of complex and interface energies of ligand-mouse $\beta$ 1AR interaction....	23
Suppl. Table 4. Quantification of conformational change in binding pocket and intracellular cavity upon ligand-mouse $\beta$ 1AR interaction. ....	23
SUPPLEMENTAL VIDEO LEGEND .....	25
Supplemental videos 1 (a-d). Metoprolol has a particular disruptive effect on neutrophil dynamics in vivo .....	25

## **SUPPLEMENTARY METHODS**

### **Mouse procedures and reagents**

All experimental and other scientific procedures with animals conformed to EU Directive 2010/63EU and Recommendation 2007/526/EC, enacted in Spanish law under Real Decreto 53/2013. Animal protocols were approved by the local ethics committees and the Animal Protection Area of the Comunidad Autónoma de Madrid.

Adult mice were maintained under pathogen-free conditions in a temperature-controlled room and a 12-hour light-dark cycle at the CNIC animal facility. Chow diet and water were available ad libitum. IRI, thioglycolate-induced peritonitis, chemokine-induced migration transwell assays, and intravital microscopy (IVM) were performed in 8-13-week-old wild type male C57BL/6 mice. The cardioprotective and neutrophil-stunning effects of metoprolol-tartrate (M5391, Sigma) were assessed alongside the effects of two other  $\beta$ -blockers: atenolol (A7655, Sigma) and propranolol-hydrochloride (P0884, Sigma). The highest i.v. dose inducing a moderate (~15%) hemodynamic effect, determined from heart rate and left ventricular pressure, was 12.5 mg/kg for all three  $\beta$ -blockers, as it was previously described for metoprolol <sup>9</sup> (**Suppl. Fig. 1**). To control for dose-dependent effects, an i.v. dose of 25 mg/kg was used in selected experiments. Mouse body temperature was strictly controlled throughout experiments to prevent additional effects due to hypothermia.

### **Mouse model of myocardial ischemia–reperfusion injury**

Male 8-13-week-old mice were subjected to 45 min occlusion of the left anterior descending (LAD) coronary artery. IS, neutrophil–platelet interactions, and neutrophil infiltration were assessed 24 h after reperfusion. The I/R procedure was carried out as previously described <sup>9</sup>. Mice were anesthetized with an intraperitoneal (i.p.) injection of an anesthetic cocktail of atropine sulfate (1 mg/kg; B. Braun, 1 mg/ml), xylazine hydrochloride (20 mg/kg; Rompun Bayer, 20 mg/ml), and ketamine (100mg/kg; Anesketin Dechra, 100mg/ml). Fully anesthetized animals were intubated and temperature controlled throughout the experiment at 36.5°C to prevent hypothermic cardioprotection. An intercostal space was opened to minimize incision size and reduce wound healing time. The LAD was then ligated with a nylon 8/0 monofilament suture for 45 min. Total coronary artery occlusion (ST-segment elevation) throughout the 45 min ischemia was confirmed

by electrocardiography (MP36R, Biopac Systems Inc.). Mice were randomized 10 min before reperfusion onset to receive a single i.v. bolus of metoprolol, atenolol, propranolol, or vehicle (0.9% NaCl; saline) via retro-orbital injection into the venous sinus. After 45 min, the suture was removed and LAD was reperfused before the intercostal space was closed. Animals were then kept with 100% O<sub>2</sub> and analgesized with subcutaneous buprenorphine (0.1 mg/kg).

### **Quantification of infarct size**

At 24 h post-reperfusion, mice were re-anesthetized and re-intubated, and the LAD coronary artery was re-occluded by ligating the suture in the same position as for the original infarction. Animals were then sacrificed and 1 ml of 1% Evans Blue dye (Sigma) was infused i.v. to delineate the area at risk (AAR, corresponding to the myocardium lacking blood flow, i.e. negative for blue dye staining). The left ventricle (LV) was isolated, cut into transverse slices (5-7 1-mm slices per LV), and both sides were imaged. To delineate the infarcted (necrotic) myocardium, slices were incubated in triphenyltetrazolium chloride (TTC, Sigma) at 37°C for 15 min. Slices were then re-photographed and weighed, and regions negative for Evans Blue staining (AAR) and TTC (infarcted myocardium) were quantified with ImageJ (NIH, Bethesda, MD). Percentage values for AAR and infarcted myocardium were independently mass corrected for each slice. % of AAR was determined as the percentage of mg:mg ratio of AAR to LV, and % of infarct size was determined as the percentage of mg:mg ratio of infarcted myocardium to AAR.

### **Myocardial neutrophil infiltration**

A group of mice underwent the IRI protocol, including randomization to receive a single i.v. bolus of saline, metoprolol, atenolol, or propranolol 10 min before reperfusion onset. Mice were sacrificed at 24 h post-reperfusion, and the LV was stored in liquid nitrogen for subsequent protein isolation and quantification. The neutrophil marker Ly6G (lymphocyte antigen 6 complex locus G6D) was detected in heart samples by immunoblotting with anti-1A8 Ly6G antibody (BE0075-1, Bioxcell).

### **Neutrophil–platelet interaction**

Neutrophil–platelet interactions were assessed in peripheral blood obtained at 24 h post-reperfusion. Blood samples were citrated and immediately included in ThromboFix Platelet

Stabilizer (6607130, Beckman Coulter, Life Sciences), which preserves platelets in their state at the time of blood extraction. After a minimum of 1 h, erythrocytes were lysed with hypotonic buffer (Red Blood Lysis buffer). Platelets (CD41<sup>+</sup> cells) and neutrophils (Ly6G<sup>+</sup> cells) were detected by flow cytometry, and double-positive cells (CD41-Ly6G<sup>+</sup> cells) were considered identified as neutrophil-platelet interactions. The number of CD41-Ly6G<sup>+</sup> cells was calculated relative to total Ly6G<sup>+</sup> cells.

### **Transwell assay of chemokine-induced migration**

The capacity of neutrophils to migrate toward the chemokine C-X-C motif ligand 1 (CXCL1) was assessed using a modification of the method of Villablanca et al.<sup>15</sup> (**Fig. 2a**). Briefly, blood from 8-12 wild type mice was collected and filtered through a 100 µm cell strainer (352360, Falcon), and erythrocytes were lysed with hypotonic buffer (RBL buffer). Leukocytes were pooled and resuspended in RPMI containing 10% FBS and the appropriate treatment: vehicle (PBS 1X), 10 µM metoprolol-tartrate, 10 µM atenolol, or 10 µM propranolol-hydrochloride. Transwell inserts (6.5 mm, 5.0 µm pore size; 3421, Corning Costar Corporation) were pretreated with 50 µl RPMI for 15 min and placed in 24-well-plates before seeding cells (100 µl;  $\sim 0.5 \times 10^4$ ). The lower compartments (wells) were filled with 600 µl RPMI containing 0.02 ng/µl CXCL1 (453-KC-010, R&D Systems) to induce chemoattractive movement (positive control) or with medium lacking CXCL1 to assess spontaneous migration (negative control). After incubation at 37°C and 5% CO<sub>2</sub> for 90 min, cells were collected from the lower compartment, and the number of neutrophils (Ly6G<sup>+</sup> cells) was evaluated by flow cytometry. Each independent experiment was conducted with leukocytes pooled from 8-12 animals, and each condition was run with 3-4 technical replicates. To allow comparison between experiments, in each independent experiment the migration of neutrophils treated with metoprolol, atenolol, or propranolol was normalized to the mean positive control value.

### **Thioglycolate-induced peritonitis**

The ability of β-blockers to inhibit neutrophil recruitment was assessed with a well-established model of thioglycolate-induced peritonitis<sup>9</sup> (**Fig. 2d**). Wild type mice were intraperitoneally injected with 1 ml sterile thioglycolate (BD211716) and immediately randomized to receive a single i.v. 12.5 mg/kg bolus of saline, metoprolol, atenolol, or propranolol. After 6 h, animals were sacrificed, and 2 ml PBS was intraperitoneally injected and distributed manually for 30 s to detach circulating cells that had infiltrated the peritoneum. Another 8 ml PBS was then injected to facilitate collection of the

peritoneal exudate. Exudate was collected, and 1ml samples were gently centrifuged at 200 xg 5 min, and cells were washed with PBS and incubated for 30 min with Dylight-650-conjugated anti-mouse Ly6G (Clone: 1A8, BE0075-1, Biorcell). After the incubation, cell nuclei were stained with DAPI (D8417, Sigma). All samples were filtered through a 100 µm cell strainer (352360, Falcon) before flow cytometry analysis for 60 s at constant flow. Neutrophil recruitment efficiency was calculated for each individual animal as neutrophils/ml of exudate.

### **LPS-induced acute lung inflammation**

Mice were anesthetized by i.p. injection of an anesthetic cocktail of atropine sulfate (1 mg/kg; B. Braun, 1 mg/ml), xylazine hydrochloride (20 mg/kg; Rompun® Bayer, 20 mg/ml), and ketamine (100 mg/kg; Anesketin Dechra, 100 mg/ml). Fully anesthetized animals were immediately randomized to receive a single i.v. 12.5 mg/kg bolus of vehicle, metoprolol, atenolol, or propranolol. The trachea was exposed, a catheter (Introcan Safety 22G, Braun) was inserted, and mice received an intratracheal injection of sterile lipopolysaccharide (LPS) (L2262, Sigma) at a high dose of 10 mg/kg in 25 µl PBS 1X, followed by 200 µl air to ensure deposition throughout each lung. Control (sham treated) mice received an intratracheal injection of 25 µl PBS. After the intratracheal administration, the wounds were closed, and mice were allowed to recover with free access to food and water. After 24 h, the animals were sacrificed and the lungs were lavaged with 1.5 ml cold PBS through a tracheal catheter (Introcan Safety 22G, Braun), and a total of 1 ml bronchoalveolar lavage fluid (BALF) was withdrawn from each mouse for the detection of neutrophils by flow cytometry. The right lung was then removed and fixed in 4% paraformaldehyde (PFA) for 24 h at 4°C, and the left lung was rapidly frozen in liquid nitrogen for later protein isolation and immunoblotting assays.

### **Lung processing for histology and immunofluorescence**

PFA-fixed right lungs were placed in 70% alcohol at 4°C and cut transversely into two portions. For histopathological scoring of acute lung injury (ALI), both transverse portions were dehydrated through an ethanol series, cleared in xylene, embedded in paraffin wax, cut into 5 µm sections, mounted on Superfrost Plus slides (Thermo Fisher Scientific), and stained with hematoxylin and eosin solution. Tissues were processed in the CNIC Histopathology Unit, and all slides were scanned using a NanoZoomer-2.0-RS digital slide scanner (C110730®, Hamamatsu, Japan) and visualized with NanoZoomer Digital Pathology software (Hamamatsu). ALI was scored with a semi-

quantitative system, using a 0-4 scale combining assessments of inflammatory cell infiltration of the airspace and vessel wall, alveolar congestion, hemorrhage, alveolar wall thickness, and hyaline membrane formation<sup>16,17</sup>. A score of 0 indicates no injury, 1 indicates mild injury, 2 moderate injury, 3 severe injury, and 4 very severe injury.

For double immunofluorescence for citrullinated histone 3 (citH3) and Ly6G, sections were deparaffinized and antigens were retrieved by boiling in citrate buffer. Sections were then blocked for 1 h with 3% normal goat serum in PBS containing 0.25% Triton X-100 and incubated overnight at 4°C with anti-citH3 antibody (rabbit polyclonal anti-histone 3 [citrulline R2 + R8 + R17]; ab5103, Abcam) and anti-Ly6G antibody (Dylight-650-conjugated anti-mouse Ly6G monoclonal; Clone 1A8, BE0075-1, Bioxcell). Sections were then incubated for 1 h with anti-rabbit Alexa Fluor-488 secondary antibody and counterstained with DAPI to visualize nuclei. For triple immunofluorescence, slides were first incubated as above with anti-Ly6G + anti-citH3 or with anti-Ly6G + anti-myeloperoxidase (MPO) antibody (rabbit polyclonal; ab9535, Abcam), followed by an overnight incubation with anti-neutrophil–elastase (NE) antibody (Cy3-conjugated rabbit polyclonal; bs-6982R, Bioss). Stained sections were covered with Fluoroshield (F6182, Sigma).

### **Flow cytometry**

Neutrophil migration in vitro in transwell assays, peritoneal infiltration in vivo, and presence in BALF were assessed by incubating cells with Dylight-650-conjugated anti-mouse Ly6G (Clone 1A8, BE0075-1, Bioxcell), with DAPI used to assess viability (D8417, Sigma). For the assessment of neutrophil–platelet interactions, blood was fixed with ThromboFix Platelet Stabilizer (6607130, Beckman Coulter Life Sciences), which can be used in conjunction with dye-conjugated anti-platelet monoclonal antibodies for flow cytometry analysis. Neutrophil–platelet interactions were assessed by incubating cells with PE-conjugated anti-mouse CD41 (Clone MWRReg30, 12-0411-83, eBioscience) and Dylight-650-conjugated anti-mouse Ly6G, with DAPI used to assess viability.

Neutrophils were gated on the basis of Ly6G<sup>+</sup> staining and were counted with a FACS Canto-3L flow cytometer equipped with DIVA software (BD Biosciences). Neutrophil–platelet interactions were identified as CD41<sup>+</sup>Ly6G<sup>+</sup> double-positive signals, quantified as a percentage of the total number of Ly6G<sup>+</sup> cells. Data were analyzed with FlowJo (Ashland) software. All experiments were conducted at the CNIC Cellomics Unit.

## **Immunoblotting**

LV and lung samples were included in RIPA buffer (containing phosphatase and protease inhibitors, Sigma) and disrupted by high-speed shaking with steel beads in a TissueLyser LT (Qiagen). Isolated proteins were quantified by Pierce BCA Protein Assay (23225, ThermoFisher Scientific), separated by SDS-PAGE, transferred to nitrocellulose membranes (Trans-Blot Turbo Transfer System, Bio-Rad), and probed with different antibodies. The presence of neutrophils in heart samples was assessed with anti-1A8 Ly6G (BE0075-1, Bioxcell). Vinculin was detected as a loading control (V4505, Sigma). H3 citrullination in lungs was detected with anti-citH3 antibody (ab5103, Abcam). GAPDH was detected as a loading control (ab8245, Abcam). After washes and incubation with appropriate secondary antibodies, bound antibodies were detected by enhanced chemiluminescence (ImageQuant LAS 4000 series, GE Healthcare Life Sciences), and blots were analyzed with ImageJ software (NIH, Bethesda, MD, USA).

## **Confocal microscopy**

To study the production of neutrophil extracellular traps (NETs), lung sections from mice with LPS-induced ALI were assessed by double immunofluorescence for citH3 and Ly6G. Images were acquired at 5 anatomical locations using a Leica TCS SP8 Confocal and gSTED 3D System fitted with an HC PL APO 63x/1.40 Oil CS2 objective (Leica Microsystems, Mannheim, Germany). The same protocol and confocal settings were used for all images and conditions. To analyze NET production, an Image J software (NIH, Bethesda, MD) Macro was designed to determine the lung-tissue area covered by cit-H3-positive and Ly6G-positive cells and the co-localization of these markers. Images from control mice (sham-treated, receiving PBS) were used to establish the intensity threshold for the Macro analysis. Lung-tissue area was quantified from bright-field images. All experiments were conducted using the confocal systems available in the CNIC Microscopy Unit.

## **Intravital microscopy**

Intravital microscopy (IVM) of the cremaster muscle microcirculation was performed after intrascrotal injection of tumor necrosis factor- $\alpha$  (TNF $\alpha$ ) (0.5 $\mu$ g, R&D Systems) <sup>4</sup> to induce local neutrophil recruitment, followed immediately by injection of a single i.v. bolus of saline, metoprolol, atenolol, or propranolol (12.5 mg/kg). Before cremaster muscle preparation, mice were

anesthetized by i.p. injection of an anesthetic cocktail of ketamine (72 mg/kg; Anesketin Dechra, 100 mg/ml) and medetomidine hydrochloride (1 mg/kg; Domitor, 1 mg/ml). Body temperature was controlled throughout the experiment to avoid possible effects due to hypothermia. After microsurgical preparation, fluorescently labeled antibodies (0.5-1.25  $\mu\text{g}/\text{mouse}$ ) were administered by retro-orbital injection into the venous sinus to label surface molecules on polarized neutrophils (FITC-conjugated anti-CD62L and allophycocyanin [APC]-conjugated anti-Ly6G) and platelets (phycoerythrin [PE]-conjugated anti-CD41). Fluorescence in cremaster muscle venules (6-10 per mouse) was acquired for 1-2 min between 210 and 300 min after TNF $\alpha$  injection (Cy3/561 nm channel for PE, FITC/488 nm channel for FITC, and Cy5/640 nm channel for APC) (**Fig. 3a, 4a**). For double staining with PE- and FITC-conjugated antibodies, acquisition was facilitated in single (FITC) and quad (PE) filters in order to avoid between-channel bleed-through of fluorescent signals.

The IVM system was built by 3i (Intelligent Imaging Innovations, Denver, CO) on an Axio Examiner Z.1 workstation (Zeiss, Oberkochen, Germany) mounted on a 3-Dimensional (3D) Motorized Stage (Sutter Instrument, Novato, CA). This set-up allows precise computer-controlled lateral movement between XY positions and a Z focusing drive for confocal acquisition. The microscope was equipped with a CoolLED pE widefield fluorescence LED light source system (CoolLED Ltd. UK) and a quad pass filter cube with a Semrock Di01-R405/488/561/635 dichroic and a FF01-446/523/600/677 emitter. We used a plan-Apochromat 40x W NA1.0  $\infty/0$  objective (Zeiss). Two-dimensional (2D) images were collected with a CoolSnap HQ2 camera (6.45 x 6.45- $\mu\text{m}$  pixels, 1392 x 1040-pixel format; Photometrics, Tucson, AZ). For confocal highspeed IVM, we used laser stacks for 488 nm, 561 nm, and 640 nm beams coupled to a confocal scanner (Yokogawa CSUX-A1; Yokogawa, Japan). 3D images were acquired at 0.55  $\mu\text{m}$  Z-intervals. Image acquisition was coordinated and offline data analysis facilitated with SlideBook software (Intelligent Imaging Innovations), run on a Dell Precision T7500 computer (Dell Inc., Round Rock, TX).

### **Tracking of crawling neutrophils**

The kinetic properties of crawling neutrophils was studied by 2D IVM. This was crucial for testing whether the differential effects of  $\beta$ -blockers on neutrophil dynamics was reflected in metoprolol-specific disruption of neutrophil kinetics. Kinetic parameters of interest were velocity, accumulated and euclidean distance, and directionality. Euclidean distance is defined as the straight-line distance between initial and finishing points of neutrophil movement, whereas accumulated distance is the total length of the path followed.



Polarized neutrophils were identified and tracked from clearly polarized morphology and uropod staining (L-selectin staining). The cell adhesion molecule L-selectin (CD62L) is expressed in a protruding microdomain at the rear of polarized leukocytes that is essential for signal integration. The CD62L-negative pole is generally known as the leading edge. Around 4-10 venules per mouse were recorded, and time-lapse videos of crawling neutrophils were analyzed with the Manual Tracking and Chemotaxis and Migration Tool plugins in ImageJ (NIH, Bethesda, MD). For each video, channel intensities were first adjusted and then converted to RGB format. Videos were rotated so that the vessels were positioned horizontally and the blood flow oriented left-to-right. Both plugins were set up with xy calibration values, which depend on the camera and microscope parameters, to convert pixels into linear measures, as well as the time interval between video frames (3 s). Each polarized neutrophil was tracked manually 21 times (1 min) using the Manual Tracking Plugin, which generated a dataset with the respective xy track coordinates. We then used the Chemotaxis and Migration Tool to plot and to obtain neutrophil kinetic parameters for the tracks: velocity ( $\mu\text{m/s}$ ), accumulated distance ( $\mu\text{m}$ ), euclidean distance ( $\mu\text{m}$ ), and directionality.

### **Neutrophil–platelet interactions**

Platelets in the inflamed cremaster were visualized as CD41-labeled cells and quantified as described elsewhere <sup>4</sup>. The uropod was defined as the CD62L-positive domain and the leading-edge as the CD62L-negative pole forming multiple protrusions and showing guided movement (Ly6G<sup>+</sup>). Between 4 and 10 venules were recorded per mouse, and neutrophil-platelet interactions at the uropod and leading edge were calculated as percentages of the total interactions.

### **3D reconstruction of polarized neutrophils**

3D IVM was used to measure 3D features of intravascular neutrophils using Imaris Software (Bitplane, Oxford). Morphological parameters of interest provided by the ImarisCell module were prolate ellipticity, sphericity, and volume. The lengths of the three semi-axes, corresponding to the Ellipsoid axis parameters, were also obtained and were used to calculate the height:length ratio. An Ellipsoid is a type of quadric that is a higher analog of an Ellipse. The lengths of the three semi-axes are fixed positive real numbers that determine the shape of the Ellipsoid. However, if 2 of these sides are equal, the Ellipsoid is a Spheroid.

3D cell reconstructions with the ImarisCell module were used to define the cell body. Regions of interest were then segmented to enclose individual polarized neutrophils (L-selectin [CD62L<sup>+</sup>] staining), thus ensuring that the reconstruction fitted the real cell structure. For reconstruction analysis, we chose the Ly6G-APC channel because Ly6G is a membrane-bound protein that gives a strong signal and allows a good rendering of cell morphology. The ImarisCell module determines the cell threshold by calculating voxel (3D pixel) intensities from the enclosed cells and comparing them with the background intensity in the enclosed sub-regions. The threshold was subsequently checked for appropriateness for all enclosed cells. As mentioned, the lengths of the 3 semi-axes, which correspond to the Ellipsoid axis parameters, were obtained to calculate the height:length ratio. The ImarisCell module reorients the enclosed cells and provides semi-axes A, B, and C that correspond to width, height, and length measurements for each of the enclosed neutrophils. Therefore, the height:length ratio was calculated as the semi-axis B:semi-axis C ratio.

### **In-silico modeling of mouse and human $\beta$ 1AR and comparative ligand docking**

For in-silico modeling of the mouse and human  $\beta$ 1AR proteins, fasta sequences (Uniprot ID: P34971 and ID: P08588, respectively) were submitted to the G-protein coupled receptor (GPCR)-I-TASSER server <sup>18</sup>. The best models corresponding to the biggest cluster (human 2580 decoys, mouse 3245 decoys, from more than 20000 in both cases) with lower energy and correct topology (seven transmembrane segments and the best structural alignment with the  $\beta$ 2AR structure (pdb ID 3sn6 as homology template) were selected as final templates. To minimize the global energy and solve some clashes in the models, the previous models were refined with the mp relax tool using the Rosetta script interface <sup>19,20</sup> of Rosetta software suite v3.10 ([www.rosettacommons.org](http://www.rosettacommons.org)). This tool recomputes the side-chain coordinates of the protein residues taking into account the membrane environment, the lipophilicity, the trans-membrane segment and the protein composition. 100 independent models were calculated for each one. As before, the models with lower energy and correct folding were selected as final models. To better show the protein position and orientation in the membrane, the refined models were submitted to the PPM server (<http://opm.phar.umich.edu/>). This server is specialized in predicting and positioning membrane proteins from 3D structures using a large structural database (membranome) and computational methods. In detail, these methods account for long-range electrostatic interactions, first-shell solvation energy (van der Waals, hydrophobic and hydrogen bond interactions), the gradual polarity changes along the bilayer normal, the preferential solvation of protein groups by water, and the hydrophobic mismatch for TM proteins <sup>21</sup>.

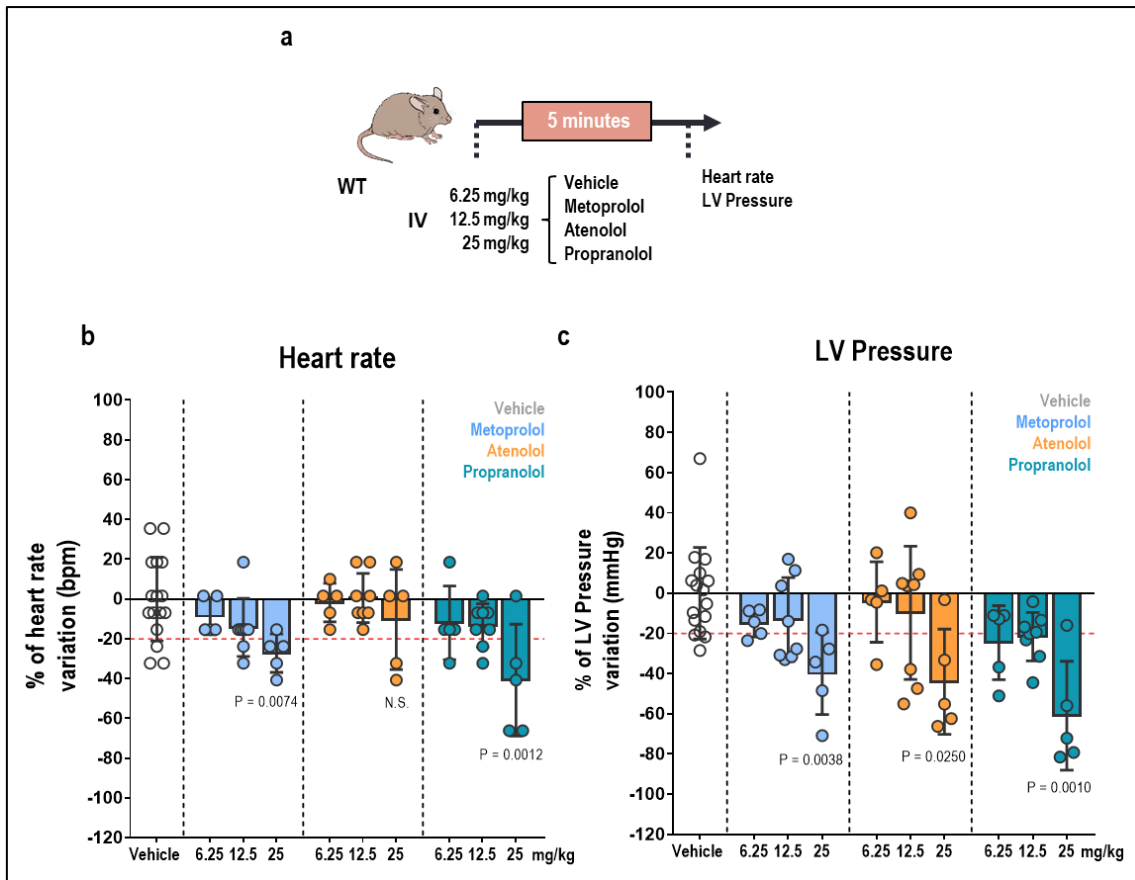
We then used the Concavity tool <sup>22</sup> to detect cavities/pockets in the models as potential ligand binding sites. The complex conformed by the final refined models with membrane positioning and the different ligands tested (epinephrine, metoprolol, atenolol and propranolol) were modeled using the ligand-docking tool from the Rosetta script of the Rosetta software suite v3.10. Briefly, a representative conformer of the ligand was located close to the ligand pocket in the receptor. The protocol computes combinations of atomic coordinates for ligand conformers and rearrangement of the side-chain (rotamers) of the residues of the receptor in the pocket, in order to explore the conformational space and find ligand-protein interactions. Finally, a new cycle of relax was made. As before, the models were submitted to the PPM server to better show the protein position and orientation in the membrane, and the pockets were analyzed with the Concavity tool. In all cases, at least 1000 models were computed. The model with correct interface topology (ligand inside the pocket without clashes between ligand and protein) and best energy of interface (minor  $\Delta G$ , more stability and interactions between protein and ligand like electrostatic, hydrophobic/hydrophilic, van der Waals and hydrogen bonds or salt bridges) were selected (**Supplemental Fig. 5**).

## **Statistics**

Data are presented as mean  $\pm$  standard deviation (SD) and were analyzed with Prism software (Graph pad, Inc.). Comparisons among the four treatments (vehicle, metoprolol, atenolol, and propranolol) were made by one-way ANOVA. P-values were adjusted with the Dunnett multiple comparisons method for data following a normal distribution and with the Dunn multiple comparisons method for data following a non-normal distribution and with the Dunn multiple comparisons method for data following a non-normal distribution. Data distribution was validated by the Shapiro-Wilk normality test. Differences were deemed statistically significant at P values below 0.05.

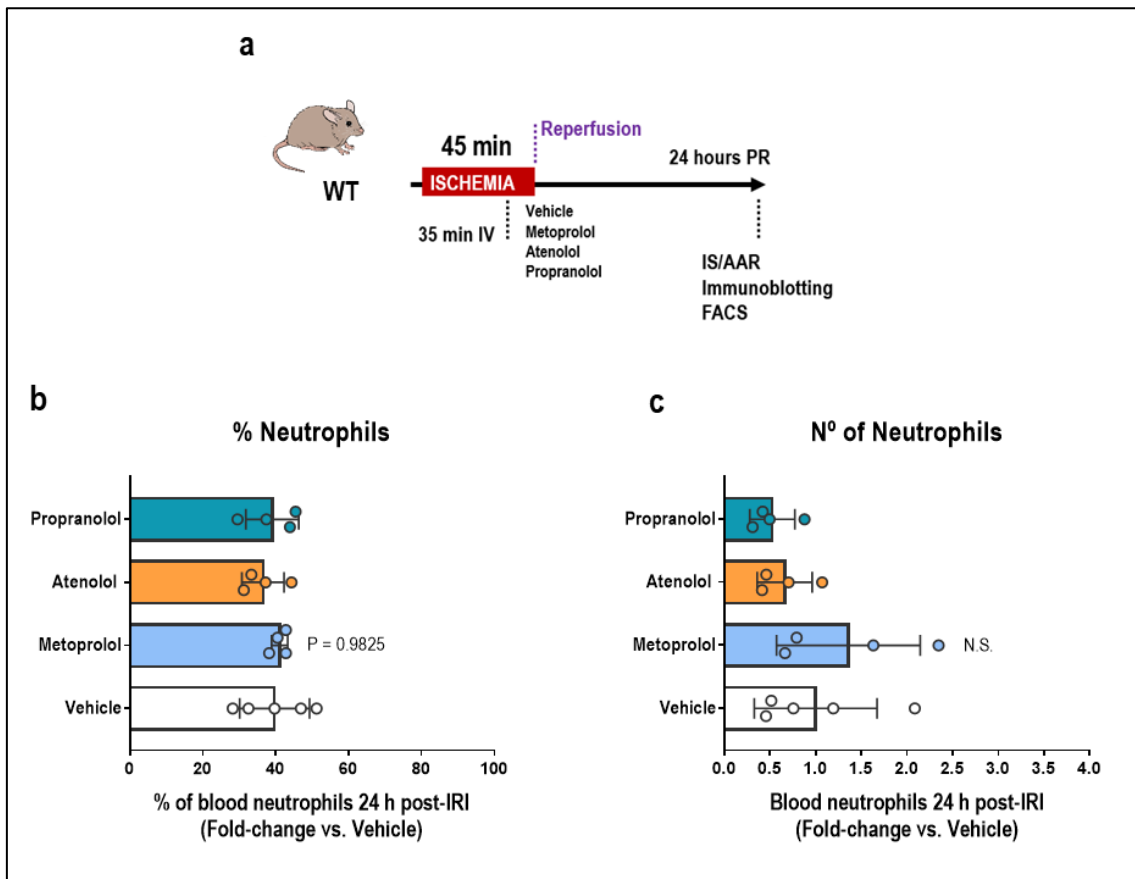
## SUPPLEMENTAL FIGURES

Supplemental Fig. 1. Dose response hemodynamic study in mice



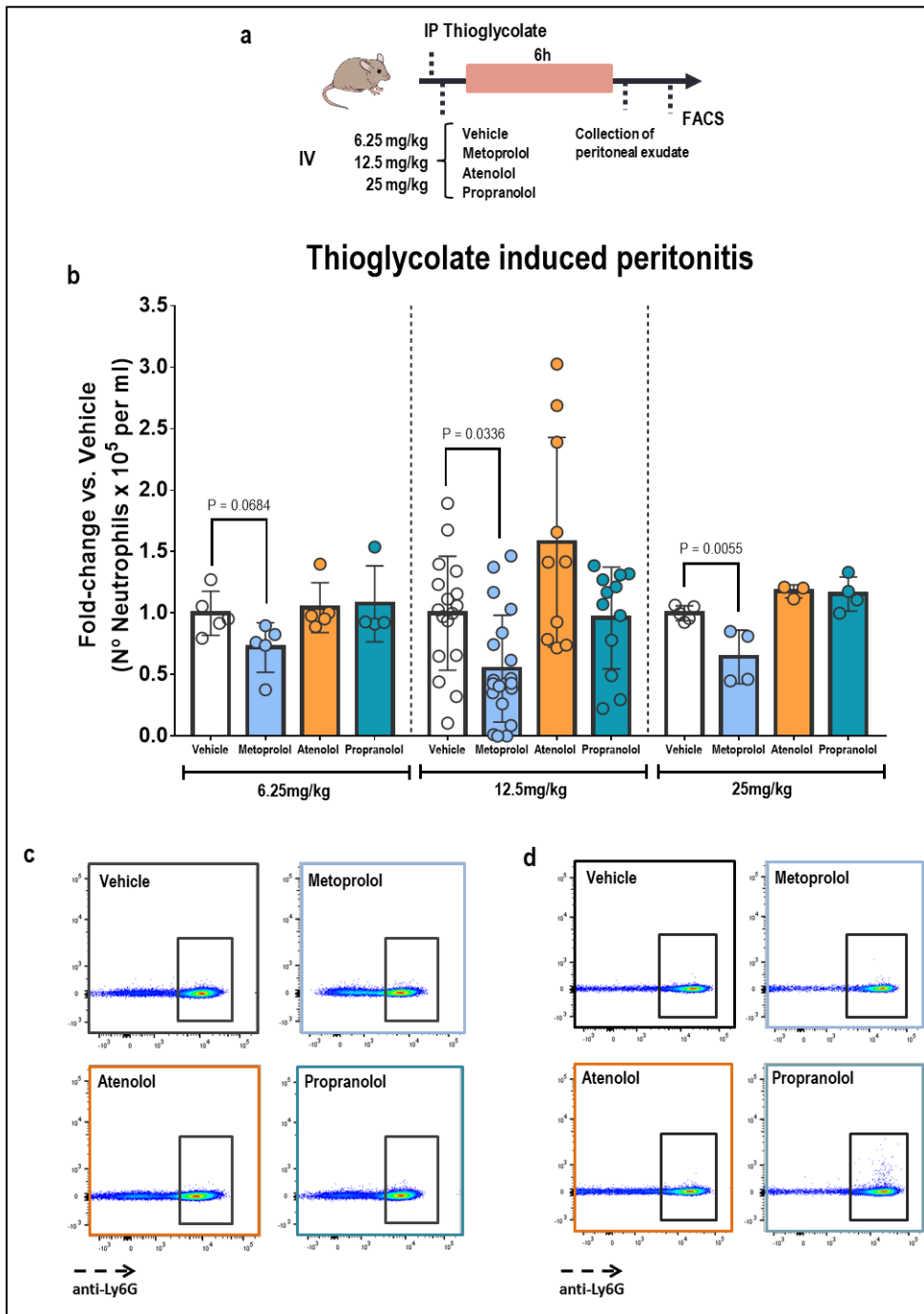
(a) Mice were anesthetized by intraperitoneal injection of an anesthetic cocktail of xylazine (20 mg/kg) and ketamine (60 mg/kg). An intravenous 6.25 mg/kg, 12.5 mg/kg and 25 mg/kg dose of metoprolol, atenolol, propranolol, or vehicle was given as a retro-orbital injection to the venous sinus. Animals were intubated and maintained at 36.5°C throughout the experiment. At 5 min after injection, an intercostal space was opened to allow measurement of hemodynamic variables. (b, c) Intravenous 12.5 mg/kg  $\beta$ -blocker induced a moderate hemodynamic effect, as indicated by decrease in heart rate (bpm) and left ventricular pressure (mmHg) of less than 20% compared to vehicle: vehicle, n=16; metoprolol, atenolol and propranolol; n=5-8 animals per treatment condition and dose. Data are presented as mean $\pm$ SD.

**Supplemental Fig. 2. Pre-reperfusion intravenous metoprolol does not affect the percentage and number of neutrophils 24 h post-IRI**



(a) Mouse model of myocardial I/R. (b, c) The percentage and number of circulating neutrophil population was not altered 24 h post-IRI by any of the 3  $\beta$ -blockers when administered pre-reperfusion: metoprolol, atenolol or propranolol.  $n=4-5$  mice per treatment condition. Data are presented as mean $\pm$ SD.

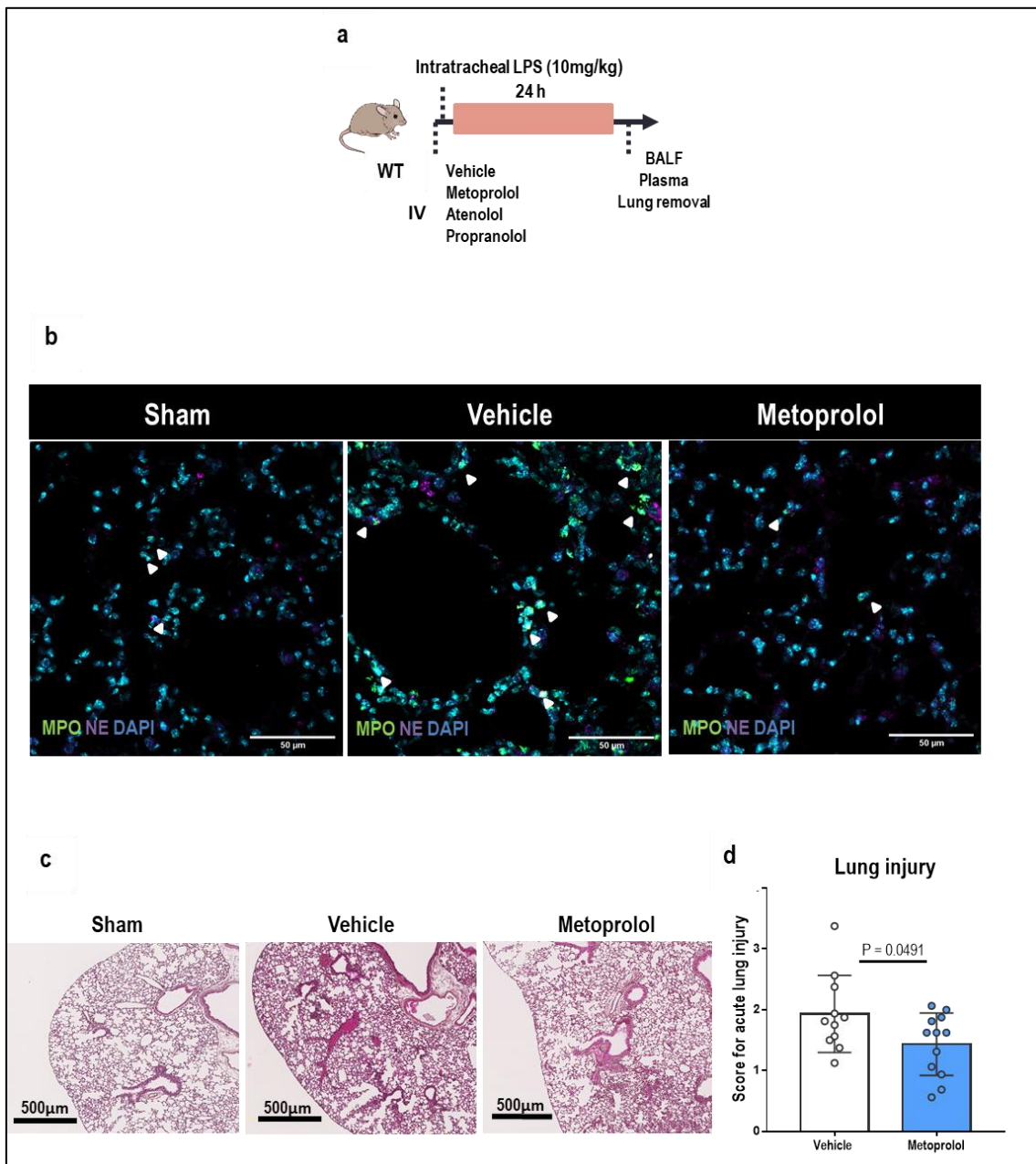
**Supplemental Fig. 3. The lack of effect on neutrophils of atenolol and propranolol is not dose-dependent**



(a) Experimental scheme for thioglycolate-induced peritonitis. Mice received a 6.25 mg/kg and 25 mg/kg i.v.  $\beta$ -blocker dose immediately after i.p. thioglycolate administration. (b, c) Flow cytometry analysis neutrophils in peritoneal exudate. (b) Absolute numbers of neutrophils detected per ml of infiltrate 6 h after thioglycolate injection was represented as a fold-change compared to vehicle. (c)

Representative flow cytometry plots illustrating reduced peritoneal infiltration of neutrophils (Ly6G+ cells) in metoprolol-treated mice. n=3-5 animals/ treatment condition and dosage. Data are presented as mean±SD..

**Supplemental Fig. 4. Metoprolol reduces MPO and ameliorates ALI**

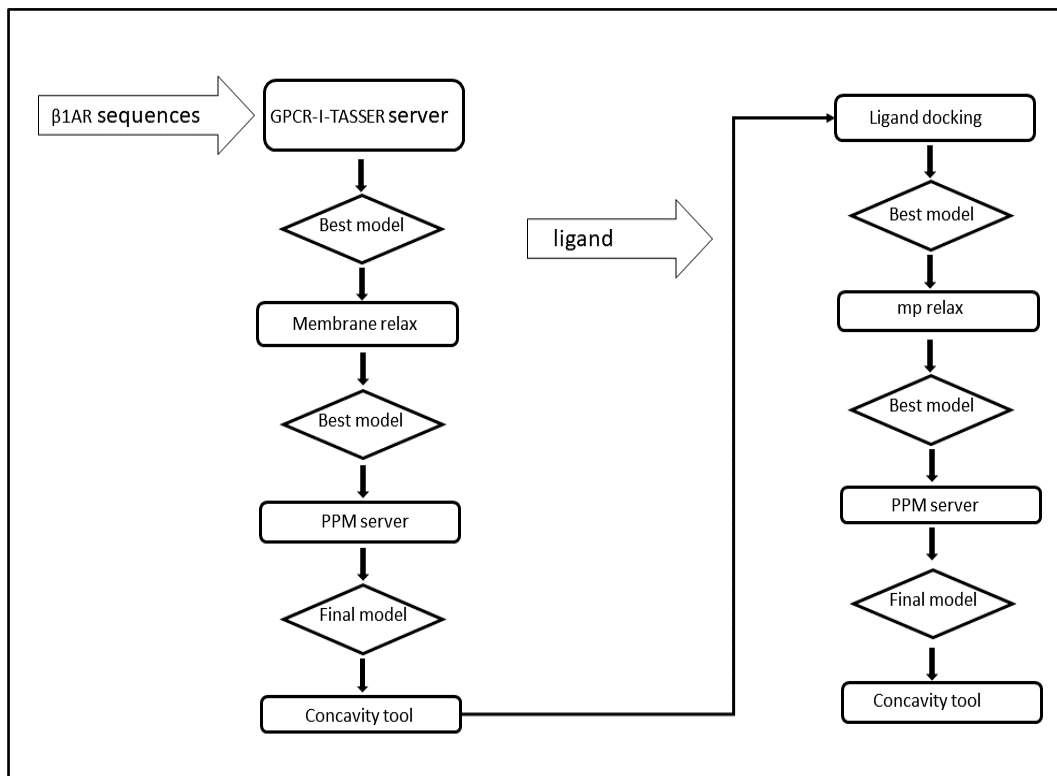


(a) Model of LPS-induced acute lung injury (ALI). Mice received an intratracheal instillation of LPS immediately after i.v. injection with the indicated treatments. (b) Representative confocal immunofluorescence of lung sections 24 h after LPS instillation, showing reduced levels of the neutrophil granule proteins MPO (green) and NE (purple) in metoprolol-treated mice. Arrowheads mark MPO and NE co-localization, indicating NET generation. (c) Representative hematoxylin and eosin stained lung sections from sham-operated mice (Control; no LPS) and vehicle- and

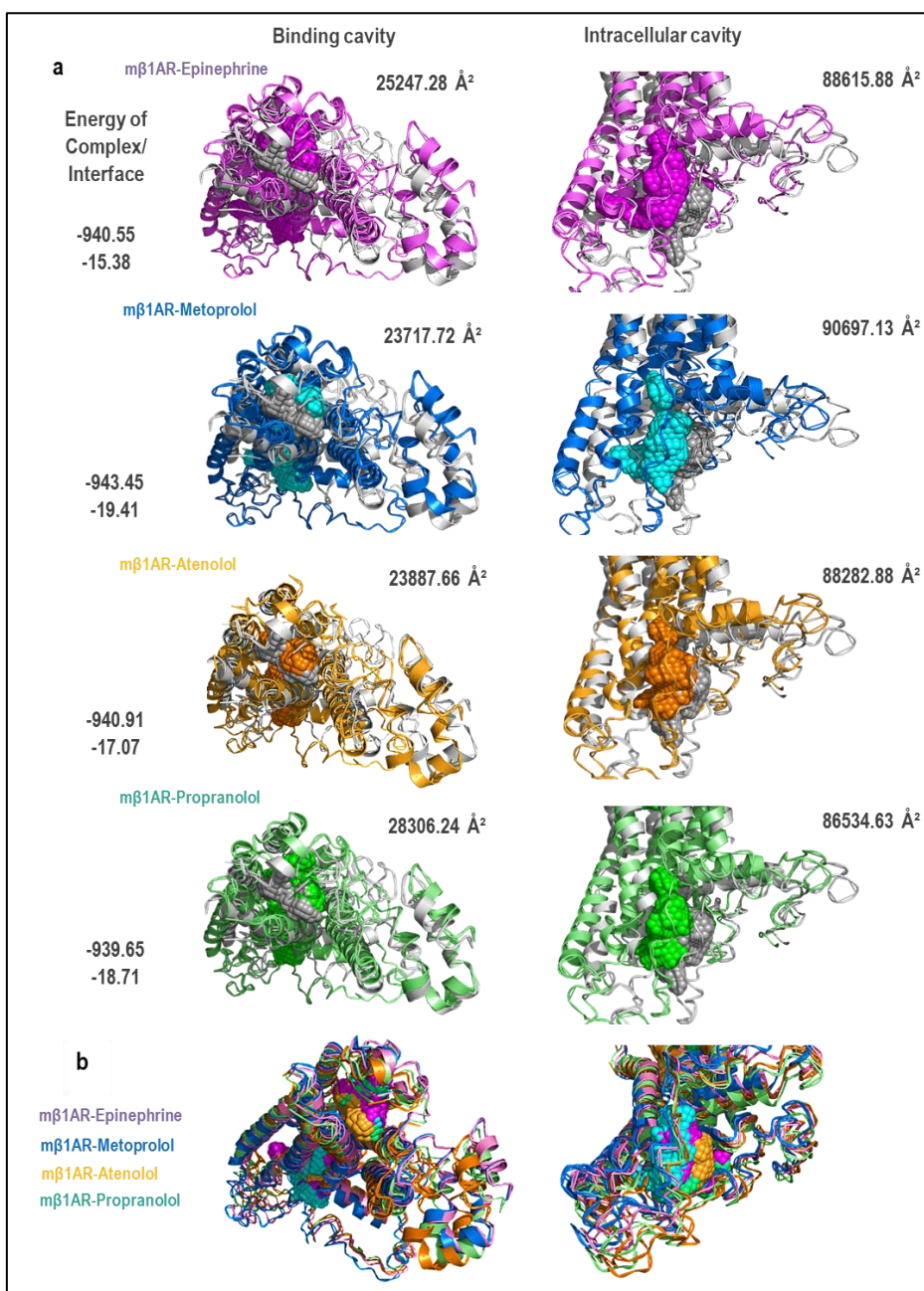


metoprolol-treated mice. (d) Lung injury was scored from 0 to 4: a score of 0 indicates no injury, 1 indicates mild injury, 2 moderate injury, 3 severe injury, and 4 very severe injury (see Methods). n=11-12 mice/condition. Data are presented as mean±SD.

**Supplemental Fig. 5. Bioinformatics Pipeline for the in-silico model of the mouse and human  $\beta$ 1AR proteins and for the simulation of the docking of these models with four ligands: epinephrine, metoprolol, atenolol or propranolol.**



**Supplemental Fig. 6. Metoprolol induces a conformational change in mouse  $\beta$ 1AR that increases the size of the intracellular cavity**



(a) Modeling of the mouse  $\beta$ 1AR modeling alone (gray) and bound to epinephrine (purple), metoprolol (blue), atenolol (orange), or propranolol (green). Each ligand-bound  $\beta$ 1AR conformation was compared to the unbound  $\beta$ 1AR conformation. Images were obtained with the PyMOL molecular visualization system. In silico analysis indicates that  $\beta$ 1AR conformational changes induced by metoprolol binding differ from those induced by the other ligands, producing an enlarged

intracellular receptor cavity that is more open than that of the epinephrine-, atenolol-, or propranolol-bound receptor. The detected changes are proportionally similar to those obtained in modeling of the human  $\beta$ 1AR (see Figure 6). (b) Superposition of all ligand-induced  $\beta$ 1AR conformations. The energies of the complex and interface are shown in Rosetta Energy Internal Units, whereas cavity sizes are shown in square Ångström Units ( $\text{Å}^2$ ).

## SUPPLEMENTAL TABLES

Suppl. Table 1. Quantification of complex and interface energies of ligand-human  $\beta$ 1AR interaction

Human $\beta$ 1AR	Energy of complex	Energy of interface
$\beta$ 1AR-Epinephrine	-1265.68	-13.65
$\beta$ 1AR-Metoprolol	-1263.64	-19.57
$\beta$ 1AR-Atenolol	-1268.61	-21.04
$\beta$ 1AR-Propranolol	-1279.98	-19.20

Suppl. Table 2. Quantification of conformational change in binding pocket and intracellular cavity upon ligand-human  $\beta$ 1AR interaction.

Human $\beta$ 1AR	Binding cavity	Intracellular cavity
$\beta$ 1AR	77377.13 Å <sup>2</sup>	39022.18 Å <sup>2</sup>
$\beta$ 1AR-Epinephrine	65470.79 Å <sup>2</sup>	37571.32 Å <sup>2</sup>
$\beta$ 1AR-Metoprolol	52117.21 Å <sup>2</sup>	63759.34 Å <sup>2</sup>
$\beta$ 1AR-Atenolol	59857.18 Å <sup>2</sup>	50069.59 Å <sup>2</sup>
$\beta$ 1AR-Propranolol	54413.68 Å <sup>2</sup>	44371.77 Å <sup>2</sup>

Metoprolol binding to human  $\beta$ 1AR induces a conformational change that increases the size of the intracellular cavity more than is achieved upon binding of epinephrine, atenolol, or propranolol. As expected, the drug-binding cavity has a minor solvent accessible surface with ligands.  $\beta$ -blockers binding to  $\beta$ 1AR have similar complex and interface energies, suggesting similar binding stabilities. Complex and interface energies are shown in Rosetta Energy Internal Units, whereas binding and intracellular cavity sizes are shown in square Ångström Units (Å<sup>2</sup>).

Suppl. Table 3. Quantification of complex and interface energies of ligand-mouse  $\beta$ 1AR interaction

Mouse $\beta$ 1AR	Energy of complex	Energy of interface
$\beta$ 1AR-Epinephrine	-940.55	-15.38
$\beta$ 1AR-Metoprolol	-943.45	-19.41
$\beta$ 1AR-Atenolol	-940.91	-17.07
$\beta$ 1AR-Propranolol	-939.65	-18.71

Suppl. Table 4. Quantification of conformational change in binding pocket and intracellular cavity upon ligand-mouse  $\beta$ 1AR interaction.

Mouse $\beta$ 1AR	Binding cavity	Intracellular cavity
$\beta$ 1AR	27796.41 Å <sup>2</sup>	84536.63 Å <sup>2</sup>
$\beta$ 1AR-Epinephrine	25247.28 Å <sup>2</sup>	88615.88 Å <sup>2</sup>
$\beta$ 1AR-Metoprolol	23717.72 Å <sup>2</sup>	90697.13 Å <sup>2</sup>
$\beta$ 1AR-Atenolol	23887.66 Å <sup>2</sup>	88282.88 Å <sup>2</sup>
$\beta$ 1AR-Propranolol	28306.24 Å <sup>2</sup>	86534.63 Å <sup>2</sup>

Metoprolol binding to mouse  $\beta$ 1AR induces a conformational change that increases the size of the intracellular cavity more than is achieved upon binding of epinephrine, atenolol, or propranolol. Complex and interface energies are shown in Rosetta Energy Internal Units, whereas binding and intracellular cavity sizes are shown in square Ångström Units (Å<sup>2</sup>).



## **SUPPLEMENTAL VIDEO LEGEND**

**Supplemental videos 1 (a-d). Metoprolol has a particular disruptive effect on neutrophil dynamics in vivo**

2D IVM recordings showing representative crawling neutrophils (positive for Ly6G [green] and CD62L [yellow]) in inflamed cremaster muscle vessels of mice receiving i.v. vehicle (saline), metoprolol, atenolol, or propranolol. Only metoprolol disrupts neutrophil behavior, significantly reducing motility.